A Non-enzymatic Glucose Biosensor Using TA-Mn Nanoparticles

Tianxin Zheng[1], Xiaoyan Wang[2], Hao Chen[3*], Sijie Yin[1*]

1 School of Automation, Beijing Institute of Technology, Beijing 100081, China

2 School of Materials Science and Engineering, Beijing Institute of Technology, Beijing 100081, China

3 Changping No.1 High School. Beijing 102299, China

704243312@qq.com

yinsijie@bit.edu.cn

Abstract. Glucose oxidase (GOD) is widely used in biological detection, clinical medicine and other fields. However, its instability, susceptibility to deactivation, and high cost necessitate the development of a stable alternative with GOD-like properties. To this end, we prepared tannic acid manganese (TA-Mn) nanoparticles via a one-pot method. UV spectrophotometer qualitatively verified that TA-Mn nanoparticles possess GOD activity, and a further quantitative calculation using a kit method revealed an activity of 4027.375 U/g, which is 12 times the activity of industrial GOD. Fourier transform infrared and UV spectroscopy confirmed that TA-Mn nanoparticles are cross-linked products of TA and $MnCl_2$. Morphological analysis revealed a metal-organic framework structure. The nanoparticles exhibited a Z-average of 77.71 nm and a polydispersity index (PDI) of 0.123, indicating a moderately dispersed, uniform, and stable system. To assess their potential in glucose detection, we fabricated TA-Mn nanoparticle-based electrodes. Cyclic voltammetry demonstrated a linear relationship between the response current and glucose concentration ($y=-0.30x+5.37$), suggesting an adsorption-controlled glucose catalysis process. A 7-day voltammetric cycle test confirmed the electrodes' stability. In summary, TA-Mn nanoparticles, with their excellent GOD activity and stability, are promising for glucose detection.

Key Words: Glucose Oxidase Nanozyme, Tannic Acid-Manganese, Biosensor

1 Introduction

Diabetes mellitus can harm heart health, and its complications can lead to permanent injuries such as amputation and blindness[1, 2]. According to the World Health Organization, there are over 420 million people with diabetes worldwide, and an average of 1.5 million people die from diabetes every year. Meanwhile, the prevalence of diabetes among adults in China has reached 11.6%, with 50.1% of patients in the prediabetes stage[3]. The prediabetes stage is reversible, and timely treatment can prevent the onset of diabetes. Blood glucose monitoring is the most crucial method for detecting, intervening, and treating diabetes. Currently, common blood glucose monitoring methods mainly include fingertip blood sampling, venous plasma glucose testing, glycated hemoglobin testing, and glycated serum protein testing[4]. However, these traditional methods have limitations such as small data volume, discontinuity, and time-consuming and laborious processes[5]. To address these issues, it is necessary to develop a fast, inexpensive, reliable, and sensitive method for real-time blood glucose monitoring to help more patients monitor and control their blood glucose levels, thereby curbing the rising incidence of diabetes. Nevertheless, currently available continuous glucose monitoring solutions on the market are based on natural enzymes, which are susceptible to temperature, humidity, pH, and non-physiological chemicals. The lifespan of glucose sensors based on natural enzymes is generally less than 14 days, and the monitoring cost is relatively high. An alternative solution for overcoming above drawbacks is using inorganic nanomaterials to repleace nature enzyme of GOD, so that the stability of current glucose sensors can be greatly improved, while the cost can also be optimized significantly.

Tannic acid is a polyphenolic compound derived from plants, exhibiting various excellent biological properties such as high biocompatibility, biodegradability, sensitive stimulus responsiveness, and unique self-healing abilities[6, 7]. Additionally, tannic acid is rich in digallic acyl groups, enabling it to rapidly self-cross-link in water without heating, adding organic solvents, or using specific instruments, forming a stable metal ion-crosslinked tannic acid nanostructure. Meanwhile, manganese is abundant on Earth, and most manganese elements exist in the form of Mn^{2+}[8]. Solutions containing Mn^{2+} can have a pH of up to 7.5, similar to the pH of human body fluids. Moreover, manganese in the human body mainly exists in the form of Mn^{2+}, and normal intake of Mn^{2+} is not toxic[9]. The multivalent state and high spin

characteristics of Mn make it a typical Fenton-like catalyst[10, 11]. Furthermore, immunostimulants prepared based on Mn^{2+} can enhance the immunotherapy effect, and biosensors based on Mn nanomaterials exhibit higher biosafety and compatibility[12, 13]. Therefore, it is inferred that TA-Mn nanoparticles formed by the crosslinking of Mn and TA have higher catalytic stability, lower cost, and are suitable for use in the human body compared to natural enzymes. The working principle of the biosensor composed of these nanoparticles is shown in Fig. 1 below. It can catalyze the oxidation of glucose to gluconic acid and hydrogen peroxide, enabling specific recognition of glucose through the detection of characteristic products.

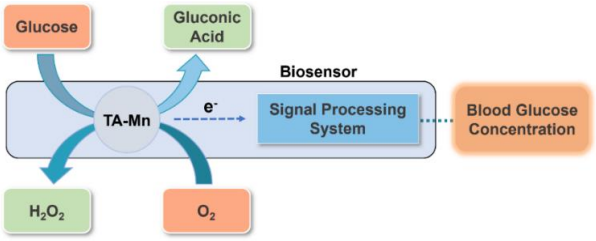

Fig. 1. Schematic figure of TA-Mn nanoparticles-based glucose sensor.

This manuscript demonstrates a new preparation process for TA-Mn nanoparticles. Compared to nanozymes, natural enzymes exhibit extremely low abundance in biological systems and pose significant challenges for purification and preservation, resulting in elevated costs for glucose sensors that rely on these natural enzymes. Furthermore, the inherent thermal and chemical instability of natural GOD renders the glucose sensors derived from it susceptible to variations in temperature, humidity, pH levels, and non-physiological chemicals. While employing precious metals for sensor fabrication can address issues related to application scope, their prohibitive cost remains a concern. Transition metal sensors offer a more economical alternative; however, they are primarily suited for alkaline environments and are not ideal for real-time monitoring of blood glucose levels in vivo. Non-metallic sensors fulfill criteria such as affordability and mild reaction conditions but suffer from limited detection sensitivity and vulnerability to interfering substances. Additionally, given the low concentration of glucose in blood plasma, accurate identification may be compromised. In contrast, utilizing nanozymes as catalysts within glucose sensors effectively addresses many of the limitations associated with previously mentioned

sensor types. Nanozymes possess enzymatic activity alongside lower costs, enhanced catalytic stability, superior selectivity, and greater ease of modification.

The activity of TA-Mn nanoparticles was quantitatively determined by a UV spectrophotometer and a test kit. Then, the synthesis mechanism and structure of TA-Mn nanoparticles were explored through Fourier transform infrared spectroscopy and UV spectroscopy. The morphology of TA-Mn nanoparticles was characterized by transmission electron microscope (TEM), scanning electron microscope (SEM), and laser particle size analyzer, proving their metal-organic framework structure and good uniformity and stability. Finally, electrochemical tests were performed to demonstrate the good stability of TA-Mn electrodes and the application potential of TA-Mn nanoparticles in glucose detection.

2 Materials and methods

2.1 Materials

Tannic acid, NaH_2PO_4 and Na_2HPO_4 were purchased from Aladdin in Shanghai. $MnCl_2$ was acquired from Bailin Wei in Beijing. Anhydrous sodium carbonate and D-(+)-glucose were acquired from Sinopharm in Beijing. 3,3',5,5'-tetramethylbenzidine (TMB) was acquired from Innochem in Beijing. Concentrated hydrochloric acid, concentrated sulfuric acid and H_2O_2 were acquired from Tongguang in Beijing. GOD Activity Detection Kit and horseradish peroxidase (HRP) were acquired from Solarbio in Beijing. Absolute methanol and ethanol were acquired from Jindong Tianzheng in Tianjin. Dimethyl Sulfoxide (DMSO) and 5 wt% nafion were purchased from Sigma-Aldrich in Shanghai. Carbon nanotubes (CNTs) was acquired from Macklin in Shanghai.

2.2. Preparation of TA-Mn Nanoparticles

TA soluiton was prepared by dissolving 17.01 mg TA into 4 mL deionized water. Adding 5 mM Na_2CO_3 solution into the TA solution for adjusting the pH to 8. Then 2.52 mg, 3.78 mg, 5.03 mg, 6.29 mg, 7.55 mg, 10.08 mg, 12.58 mg of $MnCl_2$ powder were dissolved into the prepared TA solution respectively. After stirring for 24 h, centrifuge the solution at 12000 r/min for 15 minutes at room temperature. Later, discard the supernatant and add deionized water to the centrifuge tube to evenly disperse the precipitate. Repeat the above steps for three times, then seal the centrifuge tube with parafilm and place it in a -20 °C freezer for 24 hours. After the

sample is completely frozen, poke small holes in the parafilm for ventilation, and then place the centrifuge tube in a freeze dryer for 24 hours to obtain dry TA-Mn nanoparticles.

2.3. Preparation of TA-Mn Electrode

In the manuscript, the reference electrode was Ag/AgCl, the working electrode was a glassy carbon electrode coated with TA-Mn nanoparticles, and the auxiliary electrode was a platinum sheet electrode. To acquire the TA-Mn electrode, a suede was used to polish the glassy carbon electrode firstly. After polishing, drop 1 mg/mL TA-Mn for 5 μL , CNTs for 5 μL , 1 mg/mL TA-Mn for 5 μL and 5 wt% nafion for 5 μL onto the glassy carbon surface respectively, the CNTs can improve the electron transfer ability between nanoenzymes and electrode surfaces[14]. Once the previous reagent dries, add the next solution dropwise.

2.4. Electrochemical Measurement

The type of electrochemical workstation is CHI600E, which was acquired from Chenhua in Shanghai. To measure the cyclic voltammetry curve, set the starting potential to -0.8 V, high potential to 0.8 V, low potential to -0.8 V, and ending potential to 0.8 V. Set the initial scan polarity to positive, scan rate to 0.02 V/s, sweep segments to 8, sample interval to 0.001 V, quiet time to 2 s, and sensitivity to 1. e-006 A/V. In the subsequent testing, the parameters are adjusted according to the specific content.

2.5. Model of Characterization Instrument

In addition, pH was performed by Sedolis PB-10. The sample was mixed in solution with the help of the H1085 ultrasonic water bath from Hebei Duomai, the MS-H280 Pro magnetic stirrer and the MX-S vortex mixer from SCILOGEX. Using Thermo Fisher Scientific's ST 8R and Legend Micro 17R to centrifuge the samples. Using DHP-101-1 electric heating incubator from Beijing Yongguang to achieve constant temperature incubation of samples. Measuring the particle size and dispersion of the sample by using the Zetasizer Nano zs90 laser particle size analyzer from Marvin. The morphology of the samples was characterized using the SU8010 scanning electron microscope SEM from HITACHI and the FEI Tecnai G2 F30 TEM from FEI. Use HITACHI's U-3900 for UV spectroscopy measurement, and Nicolet IS10 infrared spectrometer for infrared spectroscopy measurement. Using Perkin Elmer's

VICTOR Nivo ELISA reader to analyze the GOD activity of the sample quantitatively.

3 Results and discussion

3.1 Characterization of TA-Mn Nanoparticles

The TA-Mn nanoparticles were prepared via the aforementioned methods and detected with corresponding instruments. The size measurement results of the samples are shown in Fig. 2 (a). The measured Z-average is 77.71 nm, and the PDI of the TA-Mn nanoparticle sample is 0.123. As shown in Fig. 2 (b), the particle size distribution curve is a single peak and quite concentrated, indicating good dispersity of the prepared sample.

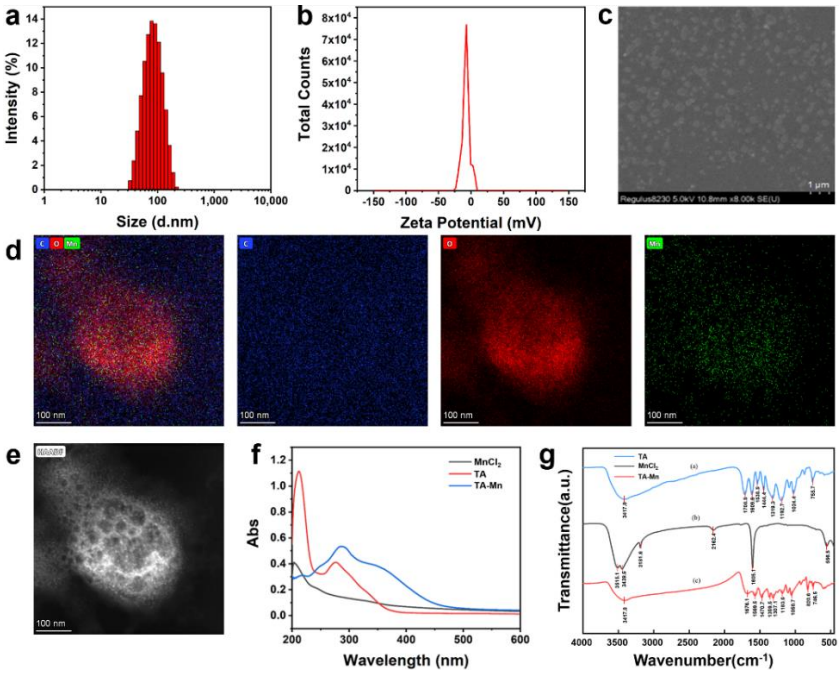

Fig. 2. Characterization of TA-Mn nanoparticles. (a) Hydrodynamic size and (b) zeta potential of TA-Mn nanoparticles. (c) SEM image of TA-Mn nanoparticles. (d) Elemental mapping of TA-Mn nanoparticles. (e) HAADF-STEM image of TA-Mn nanoparticles.(f) UV–vis absorption spectra of the aqueous solution of TA, $MnCl_2$ and TA-Mn nanoparticles. (g) FTIR spectra of TA and, $MnCl_2$ and TA-Mn nanoparticles.

The morphology of TA-Mn nanoparticles was characterized by SEM and TEM. Fig. 2 (c) shows the SEM image of TA-Mn nanoparticles, indicating that they are elliptical. Fig. 2 (d) depicts the elemental mapping of TA-Mn nanoparticles, while Fig. 2 (e) presents the High-Angle Annular Dark Field Scanning Transmission Electron Microscopy (HAADF-STEM) image of TA-Mn nanoparticles. Further characterization of the chemical composition of TA-Mn nanoparticles was carried out using corresponding Energy Dispersive X-ray Spectroscopy (EDX) from Fig. 2 (d) and HAADF imaging from Fig. 2 (e). These results confirm the presence of a metal-organic framework structure in the TA-Mn nanoparticles formed by crosslinking TA with manganese ions. The uniform elemental distribution obtained by EDX mapping indicates successful preparation of TA-Mn nanoparticles.

During the experiment, the Mn and TA content in the tested samples was controlled to be the same as the corresponding components in TA-Mn nanoparticles, to avoid experimental deviations caused by different amounts of substances. Initially, the UV-visible absorption spectra of aqueous solutions of TA, $MnCl_2$, and TA-Mn were tested. The UV absorption peak wavelength of TA generally lies between 270-300 nm[15], as shown by the red curve in Fig. 2 (f). Similarly, TA-Mn nanoparticles exhibit an absorption peak at the corresponding wavelength, indicating that the characteristic peak of TA has shifted to form a new peak in the TA-Mn nanoparticles. In Fig. 2 (g), curves a, b, and c represent the infrared spectra corresponding to TA, $MnCl_2$, and TA-Mn nanoparticles, respectively. Compared to curve a, the characteristic peaks corresponding to carbonyl groups in curve c have shifted to lower wavenumbers. Compared to curve b, the characteristic peaks of $MnCl_2$ at 3515.1 cm^{-1}, 3439.5 cm^{-1}, and 1605.1 cm^{-1} are not observed in curve c. This suggests that the formation of TA-Mn nanoparticles is due to the crosslinking reaction between TA and the manganese precursor, rather than a simple physical mixture of the two.

3.2 The Relationship between TA-Mn Nanoparticles and Their Catalytic Reaction with Glucose

β-D-glucose produces gluconic acid and H_2O_2 under the catalysis of GOD, so the enzyme activity can be analyzed by controlling the glucose concentration of the substrate to be the same and detecting the amount of H_2O_2 produced during the reaction within the same time period[16]. TMB reacts with H_2O_2 under the catalysis of HRP to produce a dimer, which is blue and has a maximum absorption peak at 652 nm[17, 18]. By comparing the height of this characteristic peak, we can determine the

H_2O_2 content in the sample, and thus infer the glucose catalytic ability of the sample. The higher the absorption peak, the stronger the catalytic ability.

TA-Mn nanoparticles were first fully dispersed in PBS at pH=7.4. Then, 0.5 mL of this dispersion was mixed with 0.5 mL of 2.5 mM glucose and incubated in a shaker at 37 °C for 70 minutes. After that, the supernatant was separated by centrifugation at 10000 r/min for 10 minutes. Next, 150 μL of 5 mg/mL TMB (dissolved in DMSO), 150 μL of 0.067 mg/mL HRP (dissolved in PBS at pH=7.4), and 300 μL of the supernatant were added to 900 μL of buffer solution at pH=4. The mixture was reacted in a 37 °C incubator for 5 minutes, and then the absorbance of the sample was measured using a UV spectrophotometer (with a cavity temperature of 37°C).

First, the GOD activity of TA-Mn nanoparticles was verified. Fig. 3 (a) demonstrates the feasibility of the above scheme through four parallel experiments and provides an initial indication that TA-Mn nanoparticles possess GOD activity. In Fig. 3 (b), when no glucose is present in the substrate, there is no characteristic peak at 652 nm, proving that the H_2O_2 in the solution originates from glucose. Subsequently, Fig. 3 (c) shows the supernatants obtained by replacing TA-Mn solution with PBS (pH=7.4), $MnCl_2$ solution, and TA solution, respectively. Among them, only the TA-Mn solution group exhibits a significant absorption peak at 652 nm and turns the solution blue. This fully demonstrates that $MnCl_2$, TA, or PBS do not significantly affect the glucose catalysis process, and it is the TA-Mn nanoparticles that play the catalytic role.

The effect of concentration on the catalytic ability of TA-Mn nanoparticles was then explored. Fig. 3 (d) illustrates the absorption peaks after the supernatants, obtained from the reaction of TA-Mn nanoparticles at concentrations ranging from 0.25 to 1.25 mg/mL with 2.5 mM glucose solution, react with TMB under HRP catalysis. As the initial concentration of TA-Mn nanoparticle solution increases, the absorption peak at 652 nm also continuously rises. This indicates that, within a certain range, the catalytic ability of TA-Mn nanoparticles is positively correlated with their concentration.

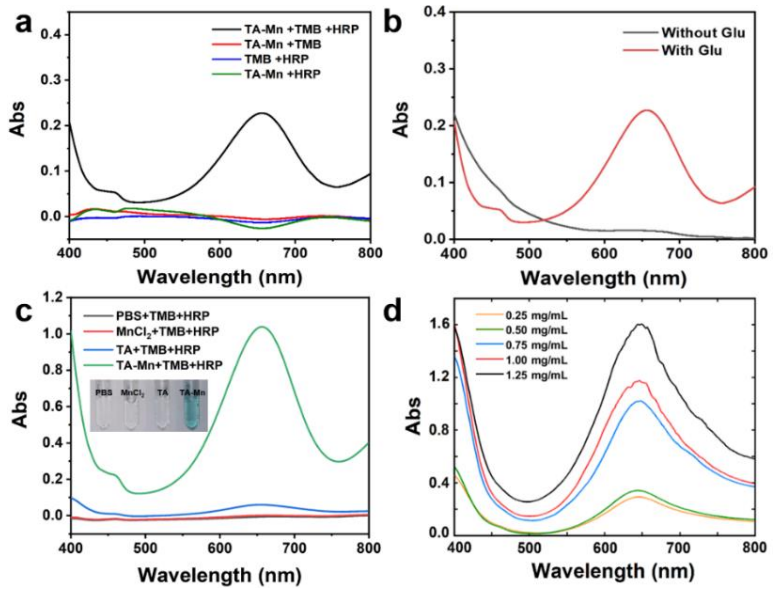

Fig. 3. Exploring the Catalytic Reaction Relationship between TA-Mn Nanoparticles and Glucose.(a) The influence of varying sample compositions on the glucose catalytic reaction. (b) The impact of glucose on the reaction. (c) Color reactions observed in different samples. (d) The relationship between the concentration of TA-Mn nanoparticles and the extent of glucose reaction.

Then, we used the microplate reader and the GOD activity assay kit to measure the activity of TA-Mn nanoparticles. The initial absorbance A1 at 20 seconds and the absorbance A2 at 2 hours and 20 seconds were recorded at a wavelength of 500 nm, and △A=A2-A1 was calculated. Then, we calculated the GOD activity, defining that one unit of enzyme activity is the amount of enzyme required to catalyze the production of 1 μmol of oxidized o-dianisidine per hour in the reaction system per gram of sample. Assuming the sample mass is W, the measurement formula is as follows:

$$GOD\ Activity\ (U/g) = 1.111 \times \triangle A \div W \quad (1)$$

The measured absorbances of each group and the calculated enzyme activities are presented in Table 1 below.

Table 1. Results of enzyme activity corresponding to different amounts of manganese.

Manganese Content (mmol)	Group	A1	A2	△A	GOD (U/g)	Average GOD (U/g)
0.02	1	0.658	0.73	0.072	799.92	555.5
	2	0.67	0.698	0.028	311.08	
0.05	1	0.71	0.758	0.048	533.28	622.16
	2	0.596	0.66	0.064	711.04	
0.1	1	0.806	0.903	0.097	1077.67	1272.095
	2	0.771	0.903	0.132	1466.52	
PBS=7	1	0.043	0.042	-0.001	-11.11	5.555
	2	0.04	0.042	0.002	22.22	

Based on the data in the previous Table 1, it can be observed that a relatively high average GOD activity is achieved when the amount of Mn precursor substance in the reaction is 0.10 mmol. Considering the difficulty in dispersing the sample at a concentration of 5 mg/mL, the sample concentrations in this experiment were set to 1 mg/mL, 2 mg/mL, and 3 mg/mL to ensure more uniform dispersion and a more stable state of the sample. The test results are presented in Table 2 below.

Table 2. Results of enzyme activity corresponding to different TA-Mn concentrations at a manganese content of 0.10 mmol.

TA-Mn Concentration (mg/mL)	Group	A1	A2	A2-A1	GOD (U/g)	Average GOD (U/g)
1	1	0.248	0.334	0.086	4777.300	4027.375
	2	0.266	0.325	0.059	3277.450	
2	1	0.429	0.460	0.031	861.025	1180.438
	2	0.381	0.435	0.054	1499.850	
3	1	0.479	0.539	0.060	1111.000	1129.517
	2	0.412	0.474	0.062	1148.033	
PBS=7	1	0.046	0.047	0.001	55.550	55.550
	2	0.044	0.045	0.001	55.550	

In both experiments, the same set of samples was tested twice, with a blank control set up to eliminate the influence of experimental factors unrelated to the test. According to the second round of test results, the average GOD activity corresponding to a TA-Mn nanoparticle concentration of 1 mg/mL was higher than that of the other two groups. Therefore, it is believed that the sample at this concentration has a stronger ability to catalyze glucose oxidation.

3.3 Preparation and Testing of Sensor Electrodes

Firstly, the effect of glucose concentration changes on the cyclic voltammetry curve was investigated. The electrolytes were PBS (pH=7.4) and glucose solutions of 1 mM, 2 mM, 3 mM, 4 mM, and 5 mM (solvent was PBS, pH=7.4). Scanning was performed at a scan rate of 0.02 V/s for 8 segments as shown in Fig. 4 (a). As the glucose concentration increased during positive voltage, the peak current value of the response current decreased, and a fitting curve as shown in Fig. 4 (b) was obtained. The coefficient of determination (R^2) of the curve was 0.97, proving that the response current value was negatively correlated with the glucose concentration, and the curve regression fit was good.

Next, the type of glucose redox reaction controlled by TA-Mn nanoparticles was investigated. The electrolyte was a 3 mM glucose solution (solvent PBS, pH=7.4), and the number of scanning segments was 8. The scan rates were sequentially changed to 0.005 V/s, 0.01 V/s, 0.02 V/s, 0.04 V/s, 0.06 V/s, 0.08 V/s, 0.1 V/s, 0.1 V/s, 0.2 V/s, 0.3 V/s, 0.4 V/s, 0.5 V/s, 0.6 V/s, 0.7 V/s, and 0.8 V/s, resulting in the curve in Fig. 4 (c). The fitting curve of the peak current value versus the corresponding scan rate is shown in Fig. 4 (d). The coefficient of determination (R^2) of the curve was 0.987, indicating a good curve regression fit. At the same time, it could be proven that the peak current was positively correlated with the scan rate, indicating that the glucose redox reaction catalyzed by TA-Mn nanoparticles was adsorption-controlled[19, 20]

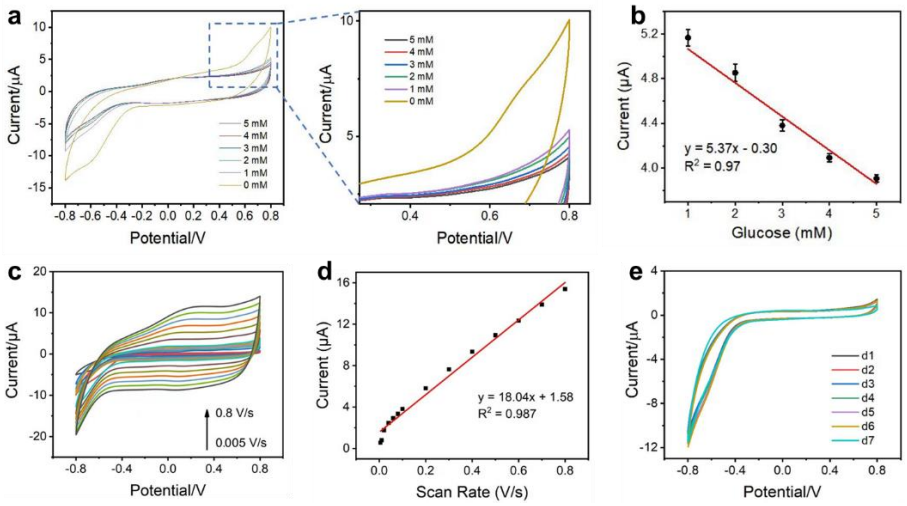

Fig. 4. TA-Mn electrode electrochemical performance results. (a) Changes in cyclic voltammetry curves with varying glucose concentration, and the peak current value at positive voltage is negatively correlated with glucose concentration. (b) The fitting curve between current and glucose concentration reflects the linear relationship between current and glucose concentration. (c) Changes in cyclic voltammetry curves with varying scan rate, the peak current is positively correlated with scanning rate. (d) i_p - υ fitting curve. (e) Cyclic voltammetry curves of the TA-Mn nanoparticle working electrode over consecutive 7 days, indicating that the working ability of the electrode is stable.

Finally, the stability of the TA-Mn nanoparticle working electrode was determined. Using a 3 mM glucose solution (solvent PBS, pH=7.4) as the electrolyte, positive scanning was performed at a scan rate of 0.02 V/s for 20 segments. The cyclic voltammetry curves of the TA-Mn nanoparticle working electrode were measured continuously for seven days, and the results are shown in Fig. 4 (e). The curves of the TA-Mn nanoparticle working electrode over seven days were basically coincident, demonstrating that the TA-Mn nanoparticle working electrode would not undergo significant denaturation within at least one week, indicating stable working ability.

4 Conclusions

Although there are various types of continuous glucose monitoring instruments on the market, their service life is generally no more than 14 days due to the inactivation and

instability of natural GOD. To address this issue, this paper prepared TA-Mn nanoparticles through a one-pot method. Qualitative verification using a UV-spectrophotometer confirmed that the TA-Mn nanoparticles possess GOD activity, and quantitative calculations using a kit method revealed that its activity is 4027.375 U/g, reaching 12 times the activity of industrial-grade GOD. UV spectroscopy and infrared spectroscopy proved that the TA-Mn nanoparticles are cross-linked products of TA and manganese chloride, and TEM was utilized to demonstrate their metal-organic framework structure. The average particle size of the TA-Mn nanoparticles was found to be 77.71 nm with a PDI of 0.123 using a laser particle size analyzer. Furthermore, electrochemical workstation tests revealed a linear relationship between the response current of the TA-Mn electrode and glucose concentration. The process of glucose catalysis by TA-Mn nanoparticles was determined to be adsorption-controlled, and the stability of the TA-Mn electrode was verified. These findings lay the foundation for the application of TA-Mn nanoparticles in glucose sensors.

Due to their advantages such as low synthesis cost, simple preparation process, stable catalytic ability, and strong controllability, the TA-Mn nanoparticles exhibit greater environmental adaptability compared to natural GOD. They are expected to replace natural enzymes and address the issues of short lifespan and high cost associated with current continuously monitorable blood glucose sensors, contributing to advancements in medical health. Additionally, with the estimated total revenue of the global nanosensor market reaching US$36.7 billion by 2026, it can be inferred that nanosensors will bring significant changes to future disease diagnosis. In this context, the TA-Mn nanoparticles with high GOD activity proposed in this paper can potentially enhance the performance of existing blood glucose sensors by integrating with novel wearable devices, implantable nanorobots, and other carriers, enabling rapid and sensitive disease diagnosis.

Disclosure of Interests. The authors declare no competing financial interests.

References

1. Pedersen, F. N., Stokholm, L., Andersen, N., et al.: Risk of Diabetic Retinopathy According to Subtype of Type 2 Diabetes. Diabetes **73**(6), 977-982 (2024)

2. Ortiz-Zúñiga, Á., Samaniego, J., Biagetti, B., et al.: Impact of Diabetic Foot Multidisciplinary Unit on Incidence of Lower-Extremity Amputations by Diabetic Foot. Journal of Clinical Medicine **12**(17), 5608 (2023)
3. Sun, H., Saeedi, P., Karuranga, S., et al.: IDF diabetes Atlas: Global, regional and country-level diabetes prevalence estimates for 2021 and projections for 2045. Diabetes Research and Clinical Practice **204**, 110945 (2023)
4. Felding, P., Jensen, I., Linnett, K., et al.: Estimation of in vivo capillary or venous blood glucose concentration from analysis on stored venous blood or its plasma and use in quality control of near-patient glucose tests. Scandinavian Journal of Clinical and Laboratory Investigation **62**(3), 201-210 (2002)
5. O'connell, J., Nathan, D. M., O'brien, T., et al.: Treatment of Diabetes — To Pump or Not to Pump. **385**(22), 2092-2095 (2021)
6. Baldwin, A., Booth, B. W.: Biomedical applications of tannic acid. Journal of Biomaterials Applications **36**(8), 1503-1523 (2022)
7. Pourmadadi, M., Omrani, Z., Abbasi, R., et al.: Poly (Tannic Acid) based nanocomposite as a promising potential in biomedical applications. Journal of Drug Delivery Science and Technology **95**, 105568 (2024)
8. Studer, J. M., Schweer, W. P., Gabler, N. K., et al.: Functions of manganese in reproduction. Animal Reproduction Science **238**, 106924 (2022)
9. Sandström, B.: Manganese in Health and Disease. The American Journal of Clinical Nutrition **60**(6), 980-981 (1994)
10. Wang, Y., Zhong, D., Xie, F., et al.: Manganese Phosphate-Doxorubicin-Based Nanomedicines Using Mimetic Mineralization for Cancer Chemotherapy. ACS Biomaterials Science & Engineering **8**(5), 1930-1941 (2022)
11. Zhong, X., Bao, X., Zhong, H., et al.: Mitochondrial targeted drug delivery combined with manganese catalyzed Fenton reaction for the treatment of breast cancer. International Journal of Pharmaceutics **622**, 121810 (2022)
12. Razumov, I., Troitskii, S., Solovieva, O., et al.: Manganese oxide nanoparticles: the influence of manganese oxidation state on selective lysis of tumor cells. Journal of Nanoparticle Research **25**(7), 140 (2023)
13. Zhang, K., Qi, C., Cai, K.: Manganese-Based Tumor Immunotherapy. Advanced Materials **35**(19), 2205409 (2023)
14. Yuwen, T., Shu, D., Zou, H., et al.: Carbon nanotubes: a powerful bridge for conductivity and flexibility in electrochemical glucose sensors. Journal of Nanobiotechnology **21**(1), 320 (2023)

15. Wiebe, H., Nguyen, P. T., Bourgault, S., et al.: Adsorption of tannic acid onto gold surfaces. Langmuir **39**(16), 5851-5860 (2023)
16. Dudkaitė, V., Kairys, V., Bagdžiūnas, G.: Understanding the activity of glucose oxidase after exposure to organic solvents. Journal of Materials Chemistry B **11**(11), 2409-2416 (2023)
17. Josephy, P. D.: Oxidative activation of benzidine and its derivatives by peroxidases. Environmental health perspectives **64**, 171-178 (1985)
18. Liu, T., Ma, M., Ali, A., et al.: Self-assembled copper tannic acid nanoparticles: A powerful nano-bactericide by valence shift of copper. Nano Today **54**, 102071 (2024)
19. Bard, A. J., Faulkner, L. R., White, H. S., Electrochemical Methods: Fundamentals and Applications. 2022.
20. Elgrishi, N., Rountree, K. J., Mccarthy, B. D., et al.: A Practical Beginner's Guide to Cyclic Voltammetry. Journal of Chemical Education **95**(2), 197-206 (2018)